A New Fast Adaptive On-Time Control for Transient Response Improvement in Constant On-Time Control

Syed Bari, *Student Member, IEEE*, Qiang Li, *Member, IEEE*, and Fred C. Lee, *Life Fellow, IEEE*

***Abstract*—These days, constant on-time current mode (COTCM) control scheme is widely used in the voltage regulator (VR) controllers because it has a higher light-load efficiency and a higher BW design capability while maintaining a simpler compensation requirement. One issue plaguing the COTCM control is its slow transient response which is caused by its fixed $T_{\rm ON}$ operation. During the heavy-load step-up transient, the duty cycle becomes saturated and the inductor current increment becomes limited by $T_{\rm ON}$ and the minimum off time ($T_{\rm OFF\_MIN}$) ratio, which can create a large undershoot at load step up. On the other hand, in the load step-down case, if the load step down occurs at the beginning of $T_{\rm ON}$, a large overshoot can be created at the output. To solve this issue, this paper presents a method designed to increase the $T_{\rm ON}$ at load step up and then very quickly, decrease at load step down in order to reduce the undershoot and overshoot at output or otherwise save the output capacitor. In this proposed method, the increase or decrease of $T_{\rm ON}$ is proportional to the output change which eliminates the chance of any overcorrection or ring-back problem unlike the methods presented in prior forums. This feature enables the control to work seamlessly in a high-frequency load repetitive case in VR applications. Since this $T_{\rm ON}$ change occurs only in the transient period when duty cycle is saturated, it does not affect the small-signal property of the COT control. Moreover, the proposed methods are very much compatible with the state-of-the-art single and multiphase COT control structures. Simulation and test results in both single and multiphase operations are also presented in the paper to verify the proposed concept.**

***Index Terms*—Adaptive on-time (AOT), constant on-time, $T_{\rm ON}$ extension, $T_{\rm ON}$ reduction, transient response.**

I. Introduction

Constant on-time control [1] is widely used for the voltage regulator (VR) applications because it has better light-load efficiency and a high-bandwidth design capability [2]. This allows us to design the control bandwidth very high in order to achieve a faster transient response. Furthermore, constant on-time control also has a smaller switching delay than peak current mode (PCM) control because of PCM control's fixed-frequency operation [3]. However, in today's world, to support the latest high-performance microprocessors and memory cards, their VRs often need to supply high-load current with a very high slew rate (up to 1000 A/μs) [4], which, as a result, urges a constant transient performance improvement in today's controls. Though widely used, COTCM control has some limitations in its load step-up and load step-down transient responses. While a fast and large load step up is applied, as shown in Fig. 1, inductor current cannot immediately increase. Therefore, until inductor current (I_L) can reach load current ($I_{\rm LOAD}$), energy demanded by load is supplied from the output capacitor which creates an undershoot at the output. Clearly, longer the inductor current will take to catch the stepped up load, the larger the undershoot will be. Microprocessor VR requires finite output impedance which makes the $V_{\rm o}$ to decrease with load current increment [4]. Their compensator design is basically a proportional gain (K) compensator to achieve adaptive voltage positioning (AVP) [5] with high-frequency pole for switching ripple attenuation. For this reason, when V_O drops very quickly at load step-up transient, V_C also goes up very quickly (shown in Fig. 1). As a result, V_C becomes higher than the inductor current sense voltage V_{IL} and this makes the general control law ineffective as the triggering of $T_{\rm ON}$ cannot start with V_C and V_{IL} intersection any more. Instead a new $T_{\rm ON}$ is generated after the minimum off time ($T_{\rm OFF\_MIN}$). From Fig. 1, it can be seen that inductor current increment is limited by the length of $T_{\rm ON}$ and $T_{\rm OFF\_MIN}$. If $T_{\rm ON}$ and $T_{\rm OFF\_MIN}$ become comparable, a large undershoot can occur at the output.

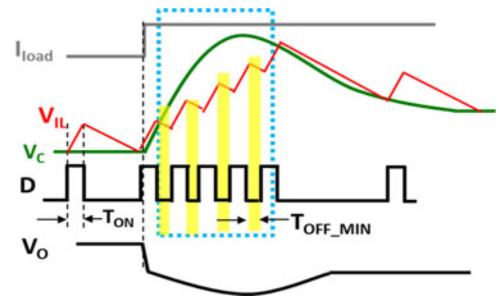

Fig. 1. Load step-up transient problem.

On the other hand, for a given power stage at the load step-down case, overshoot can be very large if load release occurs at the beginning of the $T_{\rm ON}$, which is shown in Fig. 2. Here, it shows that a load step down occurs at the beginning of the second pulse and the inductor current is expected to start decreasing right at that point However, because of the fixed $T_{\rm ON}$ time, I_L keeps increasing till $T_{\rm ON}$ expires and this extra inductor energy will be dumped in the output capacitor, and, hence, will create an overshoot at the output. It is easily understood that the value

Manuscript received November 6, 2016; revised January 31, 2017; accepted March 23, 2017. Date of publication April 12, 2017; date of current version December 1, 2017. Recommended for publication by Associate Editor T. Qian. *(Corresponding author: Syed Bari.)*

The authors are with the Center for Power Electronics Systems, Virginia Polytechnic Institute and State University, Blacksburg, VA 24061 USA (e-mail: syedbari@vt.edu; lqvt@vt.edu; fclee@vt.edu).

Color versions of one or more of the figures in this paper are available online at http://ieeexplore.ieee.org.

Digital Object Identifier 10.1109/TPEL.2017.2693382

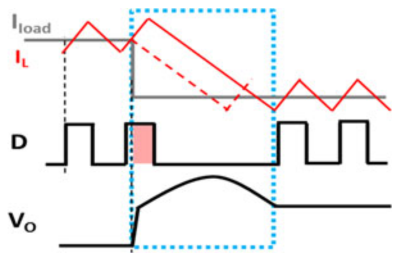

Fig. 2. Load step-down transient problem.

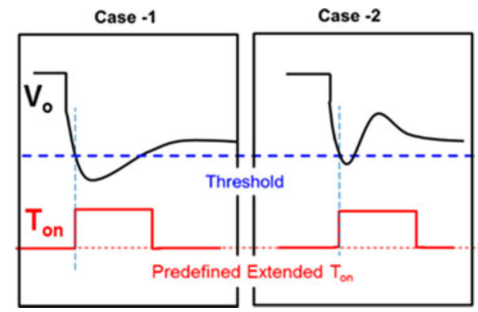

Fig. 3. Overcorrection of V_o for conventional T_{ON} extension.

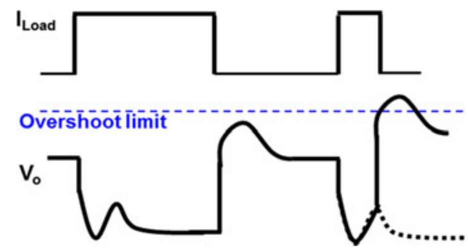

Fig. 4. Load transient overshoot problem for V_o overcorrection at load repetitive case.

of the overshoot will be higher for a larger T_{ON} if the load step down happens at the beginning of the T_{ON}.

Furthermore, constant on-time control suffers from the variation of the switching frequency (f_{SW}) with the duty cycle change. To solve this problem of variable-switching frequency, constant on time with adaptive on-time (AOT) control [6] is nowadays widely used in the VR industry. Basically, the AOT control structure is the same as the COT structure except that T_{ON} is not constant at steady state over the duty cycle range anymore. In AOT control, ideally, if T_{ON} is changed with duty cycle *D* (i.e., V_{IN} and V_{REF}) at a steady-state condition, the operating frequency will be constant over the whole duty cycle range. It can now easily be understood that instead of the switching frequency, T_{ON} of the converter will change with duty cycle. From the transient response point of view, the problem with this AOT control is that T_{ON} might become very small at the small duty cycle and become comparable to the minimum off time of the system. Therefore, the load step up at the low duty cycle operation may create a large undershoot at V_O. On the other hand, during the high duty cycle, T_{ON} can become very large and overshoot can be at its worst if the load step down occurs at the beginning of the T_{ON} period.

To improve the transient response in a buck converter, many attempts have been made so far. One method is inductor stepping or switching to increase or decrease the inductor current slope at transient instance, as shown in [7]. Another method is "capacitor charge balance," [8] which is a very good direct method of charging or discharging the output capacitor at transient instance and has good dynamic performance. However, although these variable structure controls can improve the transient by changing the inductor or injecting current in the capacitor, they also make the structure more space consuming and complex, and, hence, reduce power density of the converter. Today's VRs' power density requirements are increasing high and cannot effort additional inductors or/and switches most of the cases. In that case, improving control techniques in a simple way might be the only effective and practical solution for most of the VR applications. From control point of view, some literature improvised on sliding-mode control [9], which shows good dynamic improvements in the buck converter, but from implementation point of view, it mostly require complex digital control which is more complex and expensive than analog solutions. Among the analog solution, these days COTCM control is very popular for VR applications, and, therefore, some attempts have previously been made to improve the transient response limitations in the COTCM control. Patent US20040257056 [10] proposed a method to replace the regular T_{ON} pulses with a longer pulse when the output goes below the regulation point and the length of the longer pulse is equal to the time when output stays out of regulation. A similar concept is proposed in [11] for a multiphase operation. One problem with this method is that the over correction of V_O might cause too long of a pulse causing the inductor current to become too large and create a ring back at the output voltage. Another concept is to replace the regular T_{ON} by a predefined larger T_{ON} when undershoot occurs at load transient. This concept is presented in Patent US20130314060 [12] where output of the compensator (which compares output voltage with reference voltage) goes above the regulation point and the regular T_{ON} pulse is replaced by a predefined larger T_{ON}. Maxim integrated proposed the "extended T_{ON}" feature which is demonstrated in their controller IC [13] where T_{ON} doubles when a heavy undershoot occurs. Richtek also demonstrated a similar kind of idea in their multiphase VR controller [14]. In their control, when output goes below a certain predefined threshold voltage then all the phases turn on together and T_{ON} also becomes extended to a predefined value fixed by the user. In the VR applications, the load step and load slew rate both can vary a wide range depending of the CPU load demand. The disadvantage of this type of predefined threshold and predefined T_{ON} extension is the occurrence of "ring back" or overcorrection at V_O; for instance, if undershoot is not very large and just crossed the threshold marginally to turn on the T_{ON} extension, then there is a chance of a ring back in the output voltage, as shown in Fig. 3. It is also very difficult to determine the proper value of the threshold which will be appropriate for all value load and slew rate. For the high-frequency load repetitive case, load step down can occur very quickly after load step up. In that case, as shown in Fig. 4, V_O overshoot will be larger and it might cross the overshoot limit. That is why the "ring back" in V_O is dangerous for these VR applications.

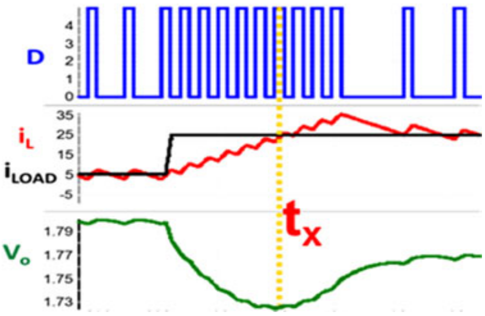

Fig. 5. Review the cause of V_o undershoot at load step up.

This paper proposes a method where $T_{\rm ON}$ extension is not fixed, but rather adaptive, with the requirement of the output voltage undershoot, and, hence, eliminates the chance of any overcorrection or ring-back problem. This paper also proposes to reduce undershoot and overshoot together while all prior research has tried to reduce undershoot only. The organization of the paper is as follows. Limitations in transient response for both load step up and down in conventional constant on-time control and the state-of-art solutions are discussed in Section I. Section II presents the concept and implementations of the proposed "fast adaptive on-time (FastAOT)" control to improve the transient response, while Section III shows analytical calculations and design guidelines for the proposed control. Experimental test results to show the transient performance improvement using this proposed method are presented in Section IV, and, finally, the conclusion is given in Section V.

II. Proposed "FastAOT" Control

A. Concept of the Proposed "FastAOT" Control

The concept of achieving the best optimized transient performance is to initiate the $T_{\rm ON}$ increase/decrease as quickly as possible after the load transient to reduce the undershoot/overshoot and also to release the $T_{\rm ON}$ extension at the right time to avoid any overcorrection. This paper proposes a method called "FastAOT" control which basically uses the derivative (dV/dt) of the V_O to increase or decrease the on time ($T_{\rm ON}$) immediately after load step up or load step down to reduce the undershoot or overshoot. Since $\mathrm{dV}_O/\mathrm{dt}$ produces a very fast detection, the V_O undershoot or overshoot at transient, as proposed in the "FastAOT" method, can initiate increase or decrease $T_{\rm ON}$ very quickly, thus reducing significant undershoot or overshoot at the output.

To achieve the proper $T_{\rm ON}$ extension in load step-up transient without any overcorrection problem, it is imperative to release the $T_{\rm ON}$ extension at the right time. For a better understanding of this transient response phenomenon at load step up, a typical undershoot case is shown in Fig. 5. Since inductor current (I_L) is smaller than load current ($I_{\rm LOAD}$) before the time instant t_x, the energy required by $I_{\rm LOAD}$ is taken from output capacitor, thus causing the output voltage (V_O) to drop. When I_L becomes equal to $I_{\rm LOAD}$, V_O becomes flat (where $\mathrm{dV}o/\mathrm{dt} = 0$). When I_L becomes higher than $I_{\rm LOAD}$, then V_O starts increasing as ($I_L - I_{\rm LOAD}$) the current is charging the output capacitor. Therefore, in order to achieve the objective of having the best optimized transient performance without any overcorrection, $T_{\rm ON}$ should be extended up to $t_{\rm x}$ point (where $I_L < I_{\rm LOAD}$) so as to reduce undershoot and stop the $T_{\rm ON}$ extension at t_x to avoid any overcorrection; after t_x, I_L is already higher than $I_{\rm LOAD}$. As proposed, the "FastAOT" method uses dVo/dt to terminate the $T_{\rm ON}$ extension, which detects the valley of V_O (where $\mathrm{dV}o/\mathrm{dt} = 0$) and eliminates any chance of overcorrection at the V_o, thus producing a very fast and optimized transient response for COT control.

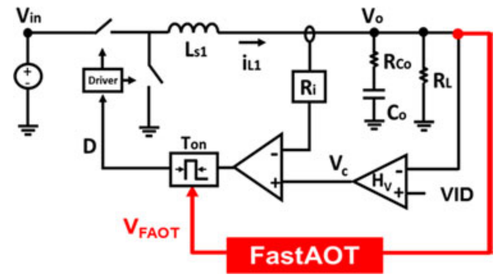

Fig. 6. Concept of the proposed "FastAOT" control.

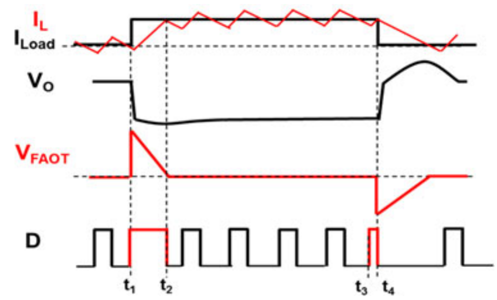

Fig. 7. Basic working principle of the proposed "FastAOT" control.

Fig. 6 shows the basic concept of the proposed method where the dV/dt block is used to create the derivative of the output voltage, called $V_{\rm FAOT}$. The FAOT signal is inserted into the $T_{\rm ON}$ generator block to increase or decrease the $T_{\rm ON}$ to reduce undershoot or overshoot. From Fig. 7, it is obvious that V_O starts decreasing right after load step up at t_1, and continues to decrease until the t_2 point, where I_L becomes equal to $I_{\rm Load}$ and starts increasing after t_2. Since dVo/dt is equal to zero at t_2, $T_{\rm ON}$ extension by using dVo/dt information will produce the maximum $T_{\rm ON}$ extension without encountering any ring-back issues. On the other hand, at the load step-down case, dVo/dt can detect the V_O change very quickly to truncate $T_{\rm ON}$, and, thus, can produce a significant V_O overshoot reduction. Hence, it can be stated that the proposed "FastAOT" control can produce fast and optimized transient response for constant on-time control.

B. Implementations of the Proposed FastAOT Control

The proposed "FastAOT" method is implemented with a conventional AOT control with $V_{\rm in}$ and $V_{\rm ref}$ sensing to change the $T_{\rm ON}$ in $T_{\rm ON}$ generator block. Implementation of the proposed "FastAOT" method can be divided into two major steps. The first step is to create the FAOT signal by using the "Proposed FastAOT" block, while the second step is to use the FAOT signal

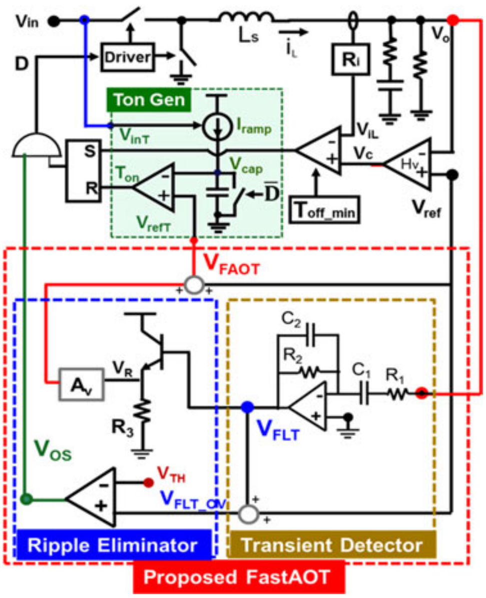

Fig. 8. Implementation for the proposed "FastAOT" control method—1.

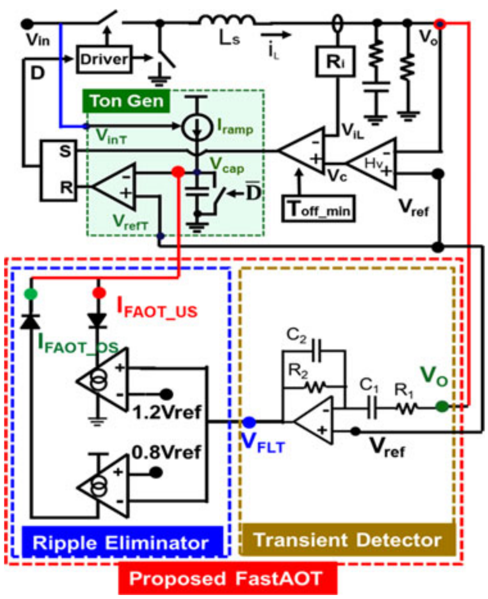

Fig. 9. Implementation for the proposed "FastAOT" control method—2.

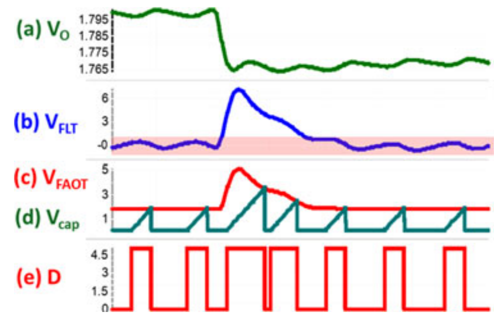

Fig. 10. Load step-up waveforms in the proposed implementation method—1.

to modify $T_{\rm ON}$ in "$T_{\rm ON}$ Gen" block. Figs. 8 and 9 show two proposed implementations methods of the FastAOT concept. In both cases, "FastAOT" block is separated into two blocks—"transient detector" and "ripple eliminator." Methods 1 and 2 basically use the same "transient detector" block but the "ripple eliminator" and the $T_{\rm ON}$ pulse modification in the "$T_{\rm ON}$ Gen" block are different. "Transient detector" is a bandpass filter which detects the change of V_o at transient to change $T_{\rm ON}$ using $\rm dV/dt$ of the V_o, but at the same time, the dV/dt of steady-state V_o ripple is also produced and may create jittering at the duty cycle. Hence, a "ripple eliminator" block is added, to eliminate the dV/dt of steady-state V_o ripple. "Transient detector" block design is a critical factor here. If a conventional differentiator is used in "transient detector" block, the dV/dt of the V_o switching ripple may still be very high to eliminate. Detailed design guidelines for the bandpass filter and ripple eliminator are given in the next chapter.

In this paper, examples of both methods are given using the dV/dt of V_o. The FAOT signal can also be created by using a dv/dt of the compensator output V_c. In comparison with V_o, V_C has less switching ripple noise than V_o, which is easier when using dV/dt but at the same time, it might be slower than V_O (depending on the compensator design) which delays the response. Since V_C is the opposite polarity of V_o, if the dVc/dt is used, then it needs to be inverted before inserting it into the $T_{\rm ON}$ generator block.

1) Details of Implementation Method—1: The load step-up response waveforms of COT control with the proposed circuit are shown in Fig. 12. When load step up occurs, V_o drop because of AVP design, as seen in curve (a) in Fig. 10. Then, the bandpass filter passes only the high-frequency part of the V_o undershoot and increases its output $V_{\rm FLT}$, as shown in curve (b) in Fig. 10. Then, in the next stage, an emitter follower is used to block the high-frequency switching ripple at $V_{\rm FLT}$, shown in curve (c) in Fig. 10, where it is seen that the red band of $V_{\rm FLT}$ around zero in curve (b) does not exist in $V_{\rm FAOT}$ in curve (c). In this way, only the peak that is created in $V_{\rm FLT}$ by the $V_{\rm out}$ undershoot will pass through this stage and will be seen at the emitter follower output $V_{\rm FAOT}$ node. Then, $V_{\rm FAOT}$ is used as the reference for the AOT generator circuit inside the green box, and, thus, peak at the $V_{\rm FAOT}$ node will increase $T_{\rm ON}$ according to the undershoot magnitude, as shown in curve (c) and (d) in Fig. 10.

In the load step-down case, when the bandpass filter in proposed, the "FastAOT" circuit detects any overshoot from the output of the converter, filters output, and $V_{\rm FLT}$ goes down very quickly. Then, this signal is compared with predetermined threshold, like 80% of $V_{\rm ref}$ is set, for example, to generate logic $V_{\rm OS}$ which eventually combined with $T_{\rm ON}$ using AND logic to expire $T_{\rm ON}$ immediately and reduce overshoot at output. In Fig. 11, the waveforms at the load step-down condition are shown. We can also observe that at the end of overshoot when V_O comes close to the regulation point, the on-time extension occurs as well. This $T_{\rm ON}$ extension helps us to eliminate the chance of any undershoot after the overshoot.

a) Optimization of method—1 for single step response at load step-up transient: The proposed method can achieve the fastest response from light load to high load in one step, as shown in Fig. 12(a) and (b), where the indictor current can

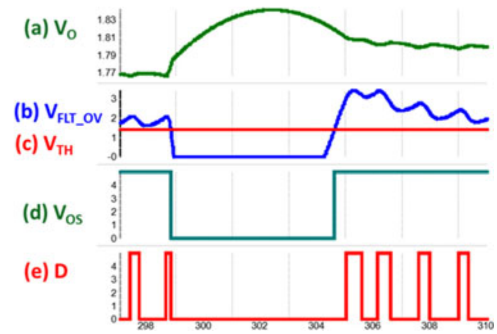

Fig. 11. Load step-down waveforms in the proposed implementation method—1.

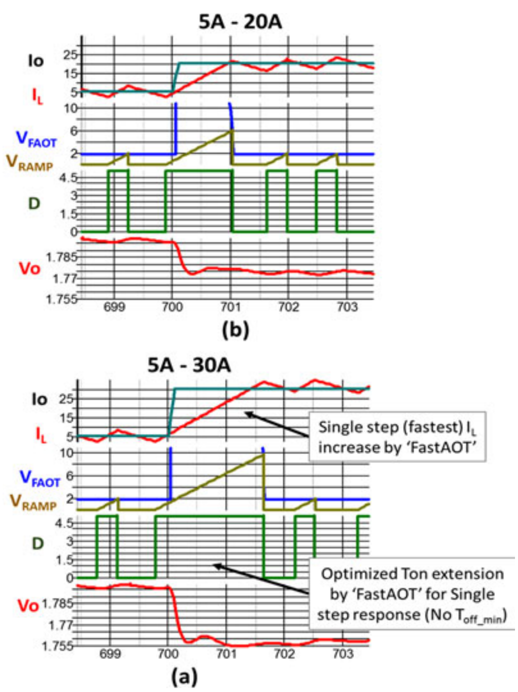

Fig. 12. Optimized "FastAOT" method—1 for single step response at load step up (a) 5–30 A. (b) 5–20 A.

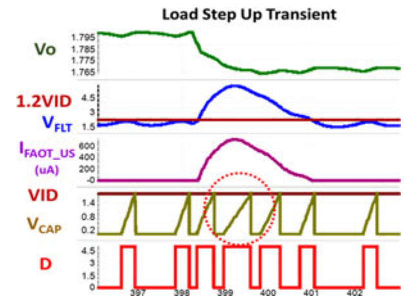

Fig. 13. Load step-up waveforms for implementation method—2.

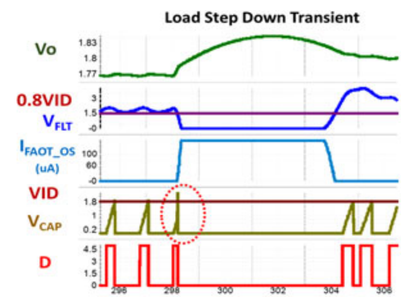

Fig. 14. Load step-down waveforms for implementation method—2.

reach from initial value to final value in one step. We can also see that there is no overcorrection as $T_{\rm ON}$ extension ends up with dV*o*/dt. To achieve this singe step response, voltage gain (Av) between $V_{\rm FLT}$ and $V_{\rm R}$ signal needs to be very high. This will make the $V_{\rm FAOT}$ signal very high at transient and $T_{\rm ON}$ will be able to extend till the transient ends, as shown in Fig. 12. Fig. 12(a) and (b) shows that single step response can be achieved smoothly in different load steps.

2) Details of Implementation Method—2: Another implementation of the proposed "FastAOT" is presented in Fig. 9, where the ramp generating current in the $T_{\rm ON}$ generator ($I_{\rm RAMP}$) is controlled to increase or decrease the on time, $T_{\rm ON}$. In Fig. 9, the proposed circuit is shown inside the red box, while the circuit implementation of $T_{\rm ON}$ generator is shown inside the green box. In this method, after detecting the undershoot or overshoot at the output voltage, the bandpass filter produces signal $V_{\rm FLT}$ in the same way implementation—1 (same "transient detector" block). Then, this $V_{\rm FLT}$ voltage signal is converted into a current by using the transconductance (G_M) amplifiers. The waveforms for the undershoot and overshoot case are shown in Figs. 13 and 14. In the load step-up case in Fig. 13, when $V_{\rm FLT}$ crosses a predefined threshold voltage (i.e., 1.2 $V_{\rm REF}$), transconductance amplifier G_{M1} generates a pulling down current ($I_{\rm FAOT\_US}$) which is subtracted from the ramp generating current ($I_{\rm RAMP}$) in the $T_{\rm ON}$ generator circuit. This will reduce the cap charging current $I_{\rm CAP}$ which will reduce the slope of the $V_{\rm CAP}$. Hence, it will increase the on time ($T_{\rm ON}$) in the $T_{\rm ON}$ generator circuit.

A load step-down case is shown in Fig. 14, where we can see that when the bandpass filter detects an overshoot in the output, the filter output $V_{\rm FLT}$ falls immediately and a push up current is generated in G_{M2} when $V_{\rm FLT}$ cross 0.8 $V_{\rm ref}$ (predefined threshold in this example). This current will be added with the original ramp generating current ($I_{\rm RAMP}$) in the $T_{\rm ON}$ generator block and increase the ramp in the $V_{\rm CAP}$ (shown by the red circle in Fig. 14) immediately to end the on time without any delay. In this way, $T_{\rm ON}$ is truncated right after an overshoot has occurred at the output to reduce the overshoot amplitude.

a) Optimization of method—2 for single step response at load step-up transient: In the proposed "FastAOT" method, the $T_{\rm ON}$ extension can be controlled by modifying the transonductance gain ($G_{\rm M}$) of the two operational tranconductance amplifiers. In Fig. 15, the key waveforms of the load step-up transient are shown with a higher $G_{\rm M1}$ value where it can be clearly seen that after transient occurs, $I_{\rm CAP}$ starts decreasing and becomes zero. Then, the $V_{\rm CAP}$ also stops increasing and becomes flat. When $V_{\rm FLT}$ starts decreasing, $I_{\rm CAP}$ and $V_{\rm CAP}$ also start increasing and at some point touch VID to end $T_{\rm ON}$. In the implementation of method—2, if a very high G_{M1} is used, then $I_{\rm FAOT\_US}$ will be very large immediately after transient occurs and the cap charging current ($I_{\rm CAP}$) will be zero or negative.

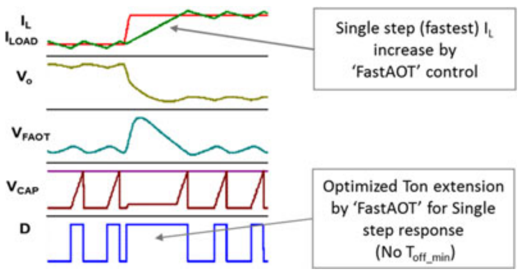

Fig. 15. Single step response at load step up in the proposed implementation method—2 for "FastAOT" control.

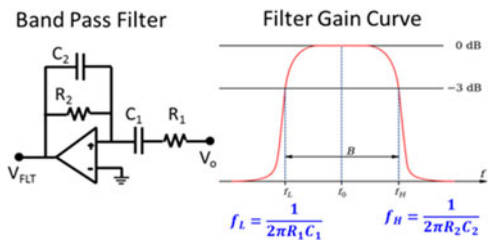

Fig. 16. Bandpass filter and its gain curve with high-and low-cutoff frequencies.

For proper operation, I_{CAP} needs to be clamp to zero to avoid the cap discharging as $I_{\mathrm{FAOT\_US}}$ is very large. When I_{CAP} will be zero, it will stop charging the cap and V_{CAP} will also be flat at that time, and, hence, will increase the T_{ON} in the T_{ON} generator circuit to achieve single step response. Fig. 15 shows the example of increasing the I_L in one step in method—2 at load step-up transient using optimized T_{ON} extension without any overcorrection.

III. Design Guideline and Performance Analysis

A. Design Guideline for "Transient Detector" and "Ripple Eliminator" Blocks

The "transient detector" block in the proposed "FastAOT" method is a bandpass filter, which allows the undershoot or the overshoot part of the output signal to pass to the next stage. From the bandpass design point of view, the objective is to maximize the pass band for the bandpass filter, but there are some limitations in maximizing this pass band. The structure of the bandpass filter and lower and higher frequency cutoff points in a bandpass filter gain curve are shown in Fig. 16.

1) Design Guideline for Setting the Higher Cutoff Frequency f_H*:* According to expression of higher cutoff frequency (f_H), it can be set by selecting R_2 and C_2 values. There is a tradeoff in setting f_H. From a design point of view f_H is desired to be set at as high a frequency as possible in order to maximize the bandwidth of the filter. However, the problem is that the output ripple at the switching frequency will also be amplified to a very large value and will be very difficult to eliminate. Therefore, f_H cannot be set very high. On the other hand, if f_H is set at very low frequency, gain for the required frequency to increase the undershoot or overshoot part of the output signal will not be high enough to increase T_{ON} significantly.

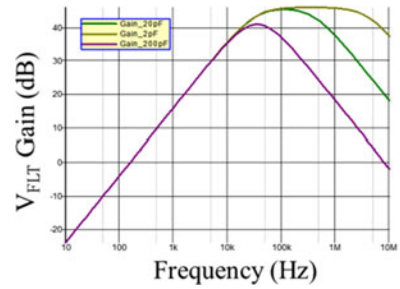

Fig. 17. Gain curve for bandpass filter with different value for C_2.

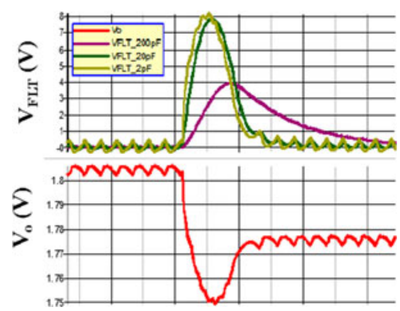

Fig. 18. V_{o} undershoot with filter output (V_{FLT}) for different value for C_2.

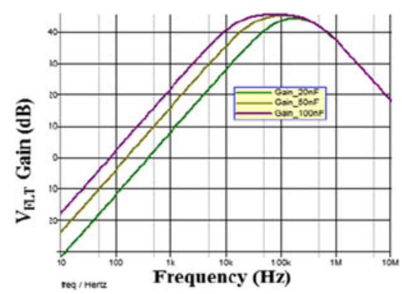

Fig. 19. Gain curve for bandpass filter with different value for C_1.

In Fig. 17, using the SIMPLIS simulator, simulation of gain curve for filter output V_{FLT} is given for different values of C_2 like 2, 20, and 200 pF with $R_2 = 20\,\mathrm{k}\Omega$, $R_1 = 100\,\Omega$, and $\mathrm{C}_1 = 50\,\mathrm{nF}$, while corresponding transient simulation results of filter output V_{FLT} for certain V_{o} undershoot are shown in Fig. 18. It can clearly be observed that the green curve with $C_2 = 20\,\mathrm{pF}$ is preferable than the other two choices as it has a high enough bandwidth to capture the undershoot properly with a reasonably lower ripple value shown in Fig. 18.

2) Design Guideline for Setting the Lower Cutoff frequency f_L*:* The lower cutoff frequency f_L can be set by selecting the capacitor C_1 and resistance R_1 in the bandpass filter. Increasing the value for the C_1, the f_L will move left toward the lower frequency and will increase the bandwidth of the bandpass filter. Hence, it is definitely desirable to set the value of C_1 as high as possible, but increasing the C_1 value has some boundaries. In Fig. 19, the output of the filter V_{FLT} has been plotted for the C_1 value = 20, 50, and 100 nF, while $R_1 = 100\,\Omega$ with $R_2 = 20\,\mathrm{k}\Omega$ and $C_2 = 20\,\mathrm{pF}$. It can be seen in Fig. 20 that amplitude of the filter output is increasing with a higher value of C_1, but at the same time because of the higher gain at the lower frequency, the settling time for the peak of V_{FLT} has

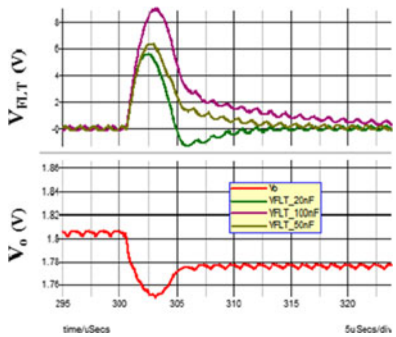

Fig. 20. V_o undershoot with filter output ($V_{\rm FLT}$) for different value for C_1.

been increased. This may keep the $T_{\rm ON}$ extension even after the undershoot is over which is not desirable. The second problem with increasing C_1 too much is that it will take more space in the board or IC. Therefore, from Fig. 20, it is clearly evident that the proper choice to set the value for C_1 will be some value between 20 and 50 nF considering other elements' value constant.

3) Design Guideline for Ripple Eliminator Block: After designing the bandpass filter properly, there should be a small enough ripple which can be easily eliminated in the ripple eliminator stage. In method—1, if the ripple amplitude is less than V_{BE}, then they can be easily eliminated. If this ripple amplitude is more than V_{BE} but less than $2\,V_{BE}$, then two cascaded transistors can be used to eliminate the ripple. For method—2, it is even easier. The threshold voltages in Op-Amp G_{M1} and G_{M2} need to be adjusted to eliminate the ripple, depending on the ripple amplitude at filter output $V_{\rm FLT}$. For example, if $G_{\rm M1}/G_{\rm M2}$ gain is set high for single step response, then ripple will also be high unless higher order bandpass filter is used. In that case, threshold voltages in "ripple eliminator" block also need to be set higher.

B. Analytical Calculation for Transient Performance Improvement in "FastAOT" Control

In this section, the analytical expression for output voltage droop for the converter is derived and by using that equation, it is also determined how much the capacitor can be saved by using the proposed method. Then, these calculations are also verified by simulation results.

B. 1) Load Step-Up Case: The equation for output voltage droop for a given load step-up case and output capacitor is given as

$$\Delta V_o = \frac{\Delta I_o^2 \times (T_{\rm on} + T_{\rm off\_min}) \times L}{2C_o \times [V_{\rm in}T_{\rm on} - V_o(T_{\rm on} + T_{\rm off\_min})]}. \qquad (1)$$

Here, ΔI_o = load step, $T_{\rm OFF\_MIN}$ = minimum off time required, and C_o = output capacitor. Now, the proposed "FastAOT" control can improve the transient by a single step response where one large $T_{\rm ON}$ can make the inductor current reach from initial load to final load level in a single step, in which case $T_{\rm OFF\_MIN}$ will be zero. In that case, equation for V_O droop will be

$$\Delta V_{o\_\rm FAOT} = \frac{\Delta I_o^2 \times L}{2C_o \times (V_{\rm in} - V_o)}. \qquad (2)$$

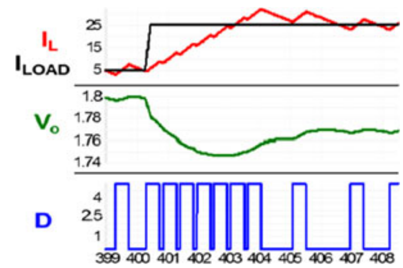

Fig. 21. Simulation results of load step-up transient without "FastAOT" control.

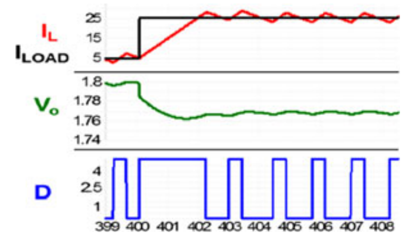

Fig. 22. Simulation results of load step-up transient for single step response with "FastAOT" control.

The proposed "FastAOT" method is simulated in a single phase VR platform [16] with AOT control with $V_{\rm in}$ and $V_{\rm out}$ sense using SIMPLIS simulator. The simulation condition is $V_{\rm in}$ = 5.2 V, V_O = 1.8 V, R_{LL} = 1.5 mΩ, $C_o = 25 \times 22\,\mu F\,(Ceramic)$, $\Delta I_{\rm LOAD}$ = 20 A, slew rate = 800 A/μs, $T_{\rm ON}$ = 432 ns, $T_{\rm OFF\_MIN}$ = 100 ns, and $f_{\rm sw}$ = 800 kHz. In Figs. 21 and 22, we see the comparison of undershoot at V_O without and with the proposed "FastAOT" method where it is clearly seen that in Fig. 22 gate signal D is immediately increased by "FastAOT" method right after the undershoot occurs and enables the inductor current I_L to catch $I_{\rm LOAD}$ very quickly compared to Fig. 21. This action eventually causes a smaller undershoot in Fig. 22 than the undershoot in Fig. 21 where $T_{\rm ON}$ was constant at transient period. The V_O droop in Fig. 21 can be calculated from (1), where we can see that at transient V_O droop is approximately 50 mV, while the steady-state error is 30 mV because of AVP. The V_O droop is calculated by using (1) which also is almost 50 mV. By using (2), we can also found the droop for a single step response which is 30 mV.

To calculate the cap saving by "FastAOT," we need to calculate how much cap will be needed to achieve a similar performance. To calculate that we can use following equation:

$$C_o = \frac{\Delta I_o^2 \times (T_{\rm on} + T_{\rm off\_min}) \times L}{2\Delta V_o \times [V_{\rm in}T_{\rm on} - V_o\,(T_{\rm on} + T_{\rm off\_min})]}. \qquad (3)$$

To achieve the same droop as with the "FastAOT" method, which is 30 mV, we find that the required capacitor will be 800 μF by using (3). Therefore, it can be said that capacitor savings will be

$$\frac{800\ \mu\text{F} - 550\ \mu\text{F}}{550\ \mu\text{F}} = 45\%.$$

2) Load step-down case: In Fig. 23, load is released at the beginning of a $T_{\rm ON}$ in the gate signal D and inductor current I_L keeps increasing because of fixed $T_{\rm ON}$. This creates additional

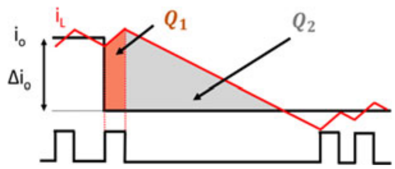

Fig. 23. Load step-down transient performance without "FastAOT" control.

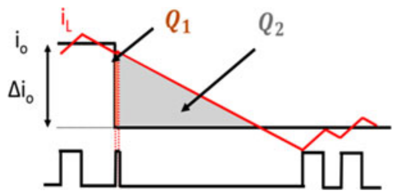

Fig. 24. Load step-down transient performance with "FastAOT" control.

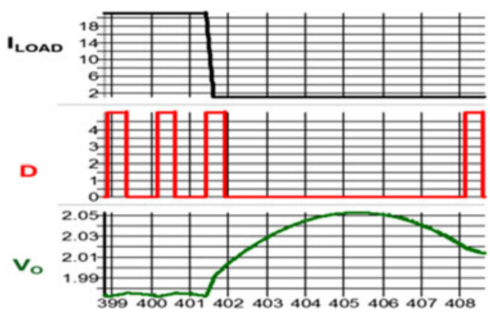

Fig. 25. Simulation results of load step-down transient performance without "FastAOT" control.

charge Q_1 in output capacitor which increases the overshot at the output. Fig. 24 shows that if the control can immediately truncate the $T_{\rm ON}$ right after load step down, only Q_2 charge will create overshoot as Q_1 is negligible compared to Q_2, which eventually will reduce overshoot. Equation (4) gives the expression for overshoot voltage at output for conventional constant on-time control, while (5) shows the case for the proposed "FastAOT" control. Clearly, overshoot in (5) is smaller as Q_2 needs to be discharged instead of $(Q1 + Q2)$

$$\Delta V_o = \frac{1}{C_o}(Q_1 + Q_2) \approx \frac{1}{C_o}\left(\Delta I_o.T_{\rm on} + \frac{\Delta I_o^2.L}{2V_o}\right) \quad (4)$$

$$\Delta V_{o\_{\rm FAOT}} \approx \frac{Q_2}{C_o} \approx \frac{1}{C_o}\left(\frac{\Delta I_o^2.L}{2V_o}\right). \quad (5)$$

To verify the load step-down case, the proposed "FastAOT" method is simulated in a single-phase VR platform using SIMPLIS simulator with same setup as load step-up case. In Fig. 25, load is released at the beginning of a $T_{\rm ON}$ in the gate signal D which aggravates the overshoot at $V_{\rm out}$. This extra amount of overshoot can be cancelled if $T_{\rm ON}$ can be expired right at the time of load release. This is done at Fig. 26 using the proposed "FastAOT" circuit. Comparing Figs. 25 and 26, we can clearly see that in Fig. 26, the gate signal D expires right after load step down, and, hence, produce a smaller overshoot. The simulation condition is same as load step-up simulation. Putting the experimental setup values in (4), overshoot is found 88.5 mV which is same as simulation results in Fig. 25. In the simulation result

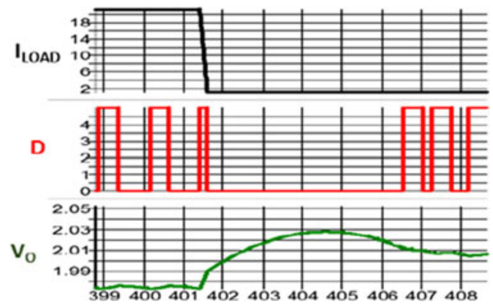

Fig. 26. Simulation results of load step-down transient performance with "FastAOT" control.

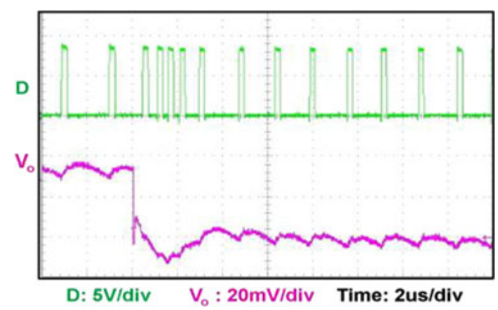

Fig. 27. Output undershoot at load step up without FastAOT control in single-phase operation.

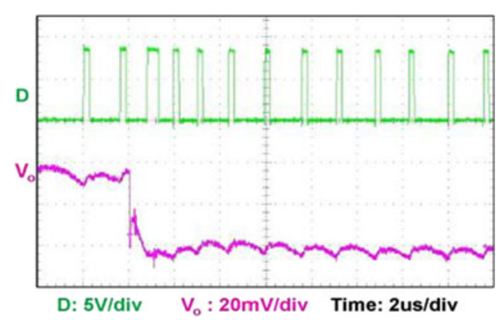

Fig. 28. Output undershoot at load step up with larger $T_{\rm ON}$ from "FastAOT" control in single-phase operation.

with "FastAOT" method, in Fig. 26, overshoot voltage reduced to approximately 60 mV. Hence, a 20-mV overshoot reduction has been achieved by the proposed "FastAOT" control. However, for higher duty cycle operation, Q_1/Q_2 ratio will be higher and will produce larger overshoot reduction in the system.

IV. Experimental Verification

In this section, the concept of "FastAOT" has been verified with experimental test results. As parasitic model for CPU socket is a significant part in load transient aspect in VR applications [16], the proposed method needed to be tested in a commercial VR platform. Therefore, to demonstrate the effectiveness of the $T_{\rm ON}$ modification by the proposed "FastAOT" concept, an experiment has been done by adding a "FastAOT" implementation method—1 circuit into a commercial VR evaluation board TPS51650 [15] through its VBAT pin. The test results for single-phase operation are shown in Figs. 27 and 28, where test condition is $V_{\rm in} = 12$ V, $V_{\rm out} = 1.05$ V, switching

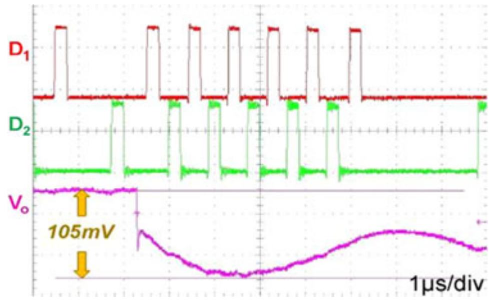

Fig. 29. Output undershoot at load step up without FastAOT control in two-phase operation.

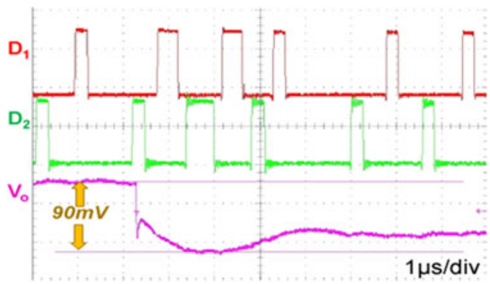

Fig. 30. Output undershoot at load step up with larger $T_{\rm ON}$ from "FastAOT" control in two-phase operation.

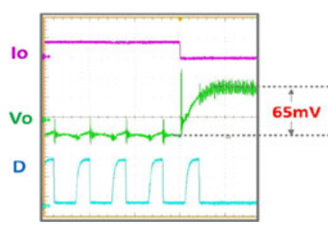

Fig. 31. Output overshoot at load step down without FastAOT control.

frequency $=$ 600 kHz, L $=$ 360 nH, Co_bulk $=$ 470 μF and Co_cer $=$ 12 $\times$ 22 μF with load step $\Delta I_{\rm LOAD}$ $=$ 17 A. It is clearly evident that in Fig. 28 where constant on time is used without the "FastAOT" method has a voltage undershoot which is eliminated in Fig. 28 where $T_{\rm ON}$ is extended by using the proposed "FastAOT" method.

To demonstrate the transient response improvement in the multiphase operation by the proposed "FastAOT" method, the same evaluation board TPS59650 is used. In the evaluation board, a two-phase operation is selected with the same test conditions as the single-phase operation except that the load step is $\Delta I_{\rm LOAD}$ $=$ 35 A in this case. A load step-up response without a proposed method is given in Fig. 29 where a 105-mV output voltage droop is seen, while the steady-state output voltage is different because of finite output impedance of VR application $\Delta V_{\rm out}$ $=$ 70 mV. Therefore, the transient undershoot is 35 mV. In Fig. 30, the same output voltage is seen with the proposed "FastAOT" method where V_O droop is 90 mV which means that the undershoot is reduced to 20 from 35 mV in the previous case.

One limitation of using the controller in TPS59650EVM is—in these two experiments as the VBAT pin of the controller is used to increase $T_{\rm ON}$, instead of modifying the $T_{\rm ON}$ generator

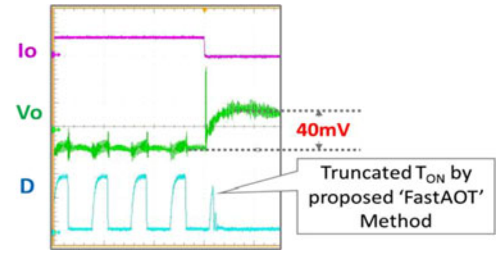

Fig. 32. Output overshoot at load step down with shorter $T_{\rm ON}$ from "FastAOT" control.

block in the controller. The $T_{\rm ON}$ extension is somewhat limited by a slow response in the VBAT pin in that case, but when this concept will be implemented in the IC level design of $T_{\rm ON}$ generator, maximum benefit of "FastAOT" will be achieved.

For load step-down case, a $\Delta I_{\rm LOAD}$ $=$ 25 A is given with same setup in EVM59650_GPU power stage where duty cycle is modified by the proposed "FastAOT" control circuit. In both cases, load step instances are tried to be kept as similar as possible to compare the effect of the proposed control. In comparison to Fig. 31, Fig. 32 shows a 25 mV (65–40 mV) overshoot reduction by $T_{\rm ON}$ truncation using "FastAOT" control at load step down.

V. Conclusion

This paper proposes a method called "FastAOT" control that increases and/or decreases the on time ($T_{\rm ON}$) immediately after load step up and/or load step down in order to reduce the output voltage undershoot and/or overshoot in constant on-time control. The main features and advantages of this proposed method are the following. 1) It can reduce both undershoot and the overshoot by changing $T_{\rm ON}$ by using one simple circuit. 2) In the proposed method, the change of $T_{\rm ON}$ is proportional to the output change, which eliminates the chance of ringing back problems, while previous works suffer from the chance of ring back with a predefined threshold and predefined $T_{\rm ON}$ increment. 3) As proposed method changes $T_{\rm ON}$ only at transient period and blocks any noise at steady state using "ripple eliminator" block, it does not affect the small-signal property of constant on-time control. 4) The proposed circuit can work with the state-of-the-art implementation of constant on time or constant on time with AOT control methods in both single and multiphase operations to improve their transient performance.

References

[1] X. Duan and A. Q. Huang, "Current-mode variable-frequency control architecture for high-current low-voltage DC-DC converters," *IEEE Trans. Power Electron.*, vol. 21, no. 4, pp. 1133—1137, Jul. 2006.

[2] Y. Yan, F. C. Lee, and P. Mattavelli, "Comparison of small signal characteristics in current mode control schemes for point-of-load buck converter applications," *IEEE Trans. Power Electron.*, vol. 28, no. 7, pp. 3405—3414, Jul. 2013.

[3] P.-L. Wong and F. C. Lee, "Switching action delays in voltage regulator modules," in *Proc. 17th Annu. IEEE Appl. Power Electron. Conf. Expo.*, 2002, pp. 675–678.

[4] VR12/IMVP7 Pulse Width Modulation Specification, Intel Corporation, 2009.

[5] K. Yao *et al.*, “Adaptive voltage position design for voltage regulators,” in *Proc. IEEE Appl. Power Electron. Conf.*, 2004, pp. 272–278.
[6] H.-C. Lin, B.-C. Fung, and T.-Y. Chang “A current mode adaptive on-time control scheme for fast transient DC-DC converters,” in *Proc. IEEE 2008 IEEE Int. Symp. Circuits Syst.*, pp. 2602–2605.
[7] X. Cao and R. Oruganti, “Fast response control of stepping inductance voltage regulator module,” in *Proc. IEEE Power Electron. Spec. Conf.*, 2005, pp. 382–388.
[8] E. Meyer, Z. Zhang, and Y. F. Liu, “An optimal control method for buck converters using a practical capacitor charge balance technique,” *IEEE Trans. Power Electron.*, vol. 23, no. 4, pp. 1802–1812, Jul. 2008.
[9] R. Venkataramanan, A. Sabanoivc, and S. Cuk, “Sliding mode control of dc-to-dc converters,” in *Proc. IEEE Conf. Ind. Electron., Control Instrum.*, 1985, pp. 251–258.
[10] J.-R. Huang, “Switching regulator with improved load transient efficiency and method thereof,” U.S. Patent 20040257056 A1, Dec. 23, 2004.
[11] J. Quintero, M. Sanz, A. Lázaro, C. Fernández, and A. Barrado, “Reduction of the switching frequency and the number of phases in multiphase VRM by applying linear—non—linear control,” in *Proc. IEEE Power Electron. Spec. Conf.*, 1985, pp. 1–6.
[12] Richtek Technology Corporation*, “Load transient of a cot mode power supply*,” U.S. Patent 20130314060 A1, Nov. 28, 2013.
[13] Maxim Integrated Products. MAX17085B Datasheet, Integrated Charger, Dual Main Step-Down Controllers, and Dual LDO Regulators, Mar. 2012. [Online]. Available: http://www.maxim-ic.com
[14] Richtek Technology Corporation. RT8888C Datasheet. 3-Phase Controller With Triple Integrated Driver for VR12.5 Mobile CPU Core Power Supply, Jul. 2015. [Online]. Available: http://www.richtek.com
[15] Texas Instruments. TPS51650A Datasheet: Dual-Channel (3-Phase CPU/1-Phase GPU) SVID, D-CAP+TM Step-Down Controllers for IMVP-7 VCORE With Two Integrated Drivers, Jan. 2012. [Online]. Available: www.ti.com
[16] Y. Ren, K. Yao, M. Xu, and F. C. Lee, “The analysis of the power delivery path from 12 V VR to the microprocessor,” in *Proc. IEEE Appl. Power Electron. Conf. Expo*, 2004, pp. 285–291.
[17] S. Bari, Q. Li, and F. C. Lee, “Fast adaptive on time control for transient performance improvement,” in *Proc. IEEE Appl. Power Electron. Conf.*, 2015, pp. 397–403.

Syed Bari (S’12) received the B.S. and M.S. degrees in electrical and electronics engineering from Bangladesh University of Engineering and Technology, Dhaka, Bangladesh, in 2004 and 2008, respectively. He is currently working toward the Ph.D. degree at the Center for Power Electronics Systems, Virginia Tech, Blacksburg, VA, USA.

He has six years of industrial experience as a Power Management System and IC Design Engineer in Bangladesh and Taiwan. His research interests include control design and modeling of dc–dc voltage regulator and point-of-load converters.

Qiang Li (M’11) received the B.S. and M.S. degrees in power electronics from Zhejiang University, Hangzhou, China, in 2003 and 2006, respectively, and the Ph.D. degree from Virginia Tech, Blacksburg, VA, USA, in 2011.

He is currently an Assistant Professor with the Center for Power Electronics Systems, Virginia Tech. His research interests include high-density electronics packaging and integration, high-frequency magnetic components, and high-frequency power conversion.

Fred C. Lee (S’72–M’74–SM’87–F’90–LF’12) received the B.S. degree in electrical engineering from National Cheng Kung University, Tainan, Taiwan, in 1968, and the M.S. and Ph.D. degrees in electrical engineering from Duke University, Durham, NC, USA, in 1972 and 1974, respectively.

He is currently a University Distinguished Professor with Virginia Tech, Blacksburg, VA, USA, and the Director of the Center for Power Electronics Systems (CPES), a National Science Foundation Engineering Research Center (NSF ERC) established in 1998, with four university partners—University of Wisconsin-Madison, Rensselaer Polytechnic Institute, North Carolina A&T State University, University of Puerto Rico-Mayagüez—and more than 80 industry members. The Center’s vision is “to provide leadership through global collaboration to create electric power processing systems of the highest value to society.” Over the ten-year NSF ERC Program, CPES has been cited as a model ERC for its industrial collaboration and technology transfer, as well as education and outreach programs. He holds 69 U.S. patents and has published 238 journal articles and more than 596 refereed technical papers. During his tenure with Virginia Tech, he has supervised to completion 71 Ph.D. and 80 Master’s students. His research interests include high-frequency power conversion, distributed power systems, renewable energy, power quality, high-density electronics packaging and integration, and modeling and control.

Dr. Lee received the William E. Newell Power Electronics Award in 1989, the Arthur E. Fury Award for Leadership and Innovation in Advancing Power Electronic Systems Technology in 1998, and the Ernst-Blickle Award for achievement in the field of power electronics in 2005. He has served as the President of the IEEE Power Electronics Society from 1993 to 1994. He was named to the National Academy of Engineering in 2011.